The Bjørntvet metabentonite: A new correlation tool for the Silurian of the southwest Oslo Region

Callum J. Hetherington, Hans Arne Nakrem & Richard A. Batchelor

Hetherington, C.J., Nakrem, H.A. & Batchelor, R.A.: The Bjørntvet metabentonite: A new correlation tool for the Silurian of the southwest Oslo Region. *Norwegian Journal of Geology*, Vol. 84, pp. 239-250. Trondheim 2004. ISSN 029-196X.

A three-layer horizon of silicate-rich rock exposed in the Bjørntvet limestone quarry in Porsgrunn has been identified as a metabentonite. Its total thickness is 75 cm, it has a dark green-grey colour and each sub-layer is 25 cm thick. Sedimentary structures are visible and there is no evidence that the siliceous material was deposited by clastic sedimentation or intruded. The boundaries between each sub-layer and the contact between the metabentonite and the limestone are conformable, sharp and depicted by bands of white calcite. The metabentonite belongs to the Steinsfjorden Formation, an Upper Silurian unit of the Oslo Region. The Steinsfjorden Formation is the youngest Wenlock unit exposed in the area and is conformably overlain by the Ringerike Group. In this area the Steinsfjorden Formation is approximately 140 m thick, and the metabentonite lies 40 m above its base. On the basis of a limited microfossil fauna, including conodonts and scolecondonts, the metabentonite is of Late Wenlock to Early Ludlow age. Each sub-layer is dominated by quartz, calcite and plagioclase, with smaller quantities of orthoclase, biotite, muscovite, chlorite, epidote, amphibole and pyroxene. This mineral assemblage grew during contact metamorphism of the rock due to emplacement of the larvikite complex to the southeast. The whole-rock chemistry of the bands suggests that they are derived from calc-alkaline dacitic magma, erupted in a volcanic arc setting. Correlation between this metabentonite and other Silurian bentonites in Norway and Scandinavia is discussed.

Callum J. Hetherington & Hans Arne Nakrem, Geologisk Museum, Universitetet i Oslo, Postboks 1172 Blindern, NO-0318 Oslo. Richard A. Batchelor, School of Geography and Geosciences, Irvine Building, University of St. Andrews, St. Andrews, Fife, KY16 9AL, Scotland, UK.

Introduction

The Steinsfjorden Formation is the youngest fully marine unit of the Silurian Wenlock series exposed in the Palaeozoic sequences of the Oslo Region. The formation consists of irregularly varying proportions of shale, marls, dolomitic shales, dolomites and limestones (Worsley et al. 1983).

A continuous section of the Steinsfjorden Formation is not exposed in any part of the Oslo Region, but numerous exposures in the Ringerike district (Fig. 1) provide overlapping sections which give a comprehensive overview of the unit (Worsley et al. 1983). The formation is also exposed at several other localities along the north-south axis of the Oslo palaeorift, including Asker, Holmestrand and Skien (Fig. 1). The unit has a maximum thickness of 260 m in the north, and progressively thins towards the south with a minimum thickness of 115 m at Holmestrand (Worsley et al. 1983).

The range of rock types exposed in the formation and their varying thicknesses reflects a non-uniform depositional environment in the Oslo region during the Wenlock period. Varying geological conditions between different geographic, but contemporaneous, localities make the application of high-resolution correlation across faunal provinces problematic. Contact metamorphism after emplacement of rift-related magmatic bodies (Fig. 1) further hinders the application of biostratigraphic methods. The metamorphism resulted in recrystallisation of many carbonate rocks, destroying much of the fossil record. Therefore, the identification of unique chronostratigraphic marker beds, exposed across the region, is invaluable for stratigraphic correlation.

The presence of numerous clay bands, identified as K-bentonites, in the Silurian rocks of Northern Europe has been well documented (Fortey et al. 1996). These rocks, with their distinctive chemical and mineralogical characteristics, provide one possible tool for correlation purposes (Batchelor & Jeppsson 1994; Batchelor & Jeppsson 1999; Batchelor et al. 1995; Kiipli et al. 2001).

A thermally metamorphosed horizon of siliceous rock deposited conformably in a unit of limestone in the Steinsfjorden Formation has been identified. Its mineralogical, textural, geochemical and stratigraphical properties are presented and its role as a possible chronostratigraphic marker bed is evaluated.

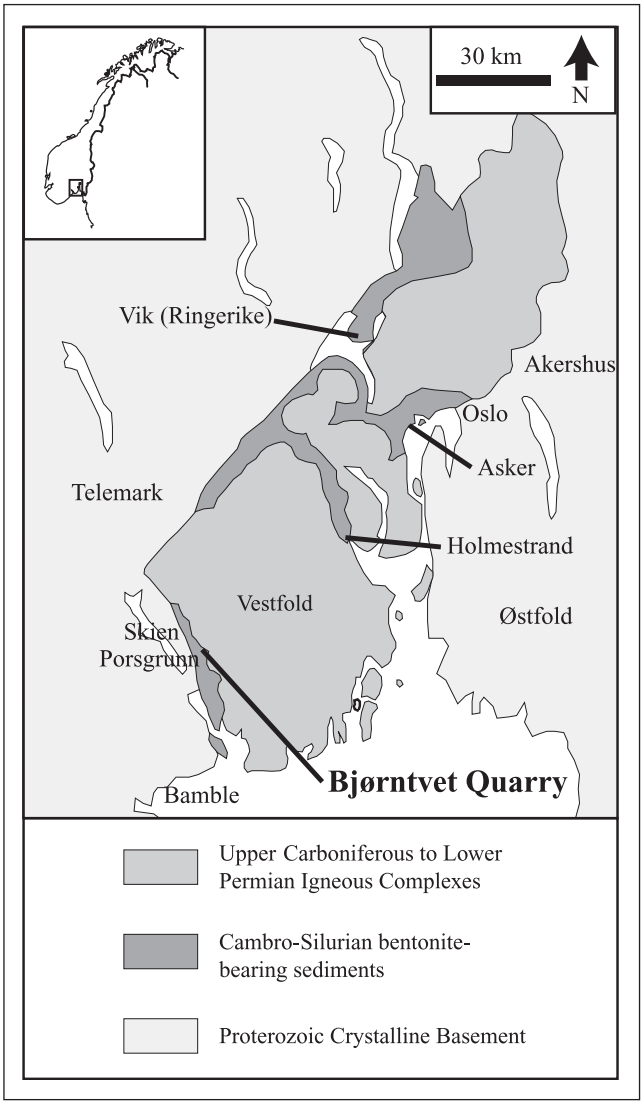

Fig.1. Map of the Oslo Region showing key exposures of the Steinsfjorden Formation.

Analytical methods

Mineral compositions were determined by electron probe microanalysis (EPMA) using the Cameca SX-100 microprobe at the University of Oslo. The electron microprobe is equipped with 5 crystal spectrometers and software by Cameca. Analyses were made with a focused electron beam (spot size = 2 μm). The accelerating voltage was 15 kV, the beam-current was 10 nA, and the counting times were 10 seconds. The electron microprobe was calibrated for each element analysed using well-characterized natural materials as standards. A PAP-type correction procedure (Pouchou & Pichoir 1984) was used for all data reduction, and detection limits were determined by measuring the just-detectable peak, corresponding to 3σ of the background count. All mineral abbreviations are after Kretz (1983).

Three samples, one from each sub-layer, were analysed for major and trace elements by XRF using standard fused glass bead and pressed powder-pellet techniques with a Philips PW1410 X-ray spectrometer (Rh tube).

Additional trace elements and rare earth elements (REE) were analysed at Activation Laboratories (Ancaster, Canada) using their *Ultratrace 1* method. A 0.5 g sample was digested in aqua regia at 90°C in a microprocessor-controlled digestion box for 2 hours. The solution was diluted and analyzed by inductively coupled plasma mass spectrometry using a Perkin Elmer SCIEX ELAN 6100. International certified reference materials USGS GXR-1, GXR-2, GXR-4 and GXR-6 were analyzed at the beginning and end of each batch of samples. Internal control standards were analyzed every 10 samples and a duplicate was run every 10 samples.

The Bjørntvet Limestone Quarry

In the south of the Oslo Region the middle sections of the Steinsfjorden Formation are dominated by particularly high quality limestone (>65 wt.% CaO). This rock is extracted for cement production in the Holmestrand and Porsgrunn regions (Fig. 1). In the latter region, the limestone in the Bjørntvet Quarry (Map sheet 1713/II. Norwegian grid reference: [32V NL 385 545]) exposes the lower 115 m of the Steinsfjorden Formation, which has a total thickness of 140 m in this area.

The exposed limestone has a NNW/SSE strike and dips gently to the ENE. Numerous palaeontological and sedimentary structures including coral reefs and cross-bedding, sand and silt lenses and very thin bands of green coloured silicate-rich rocks are preserved (Wilkinson 1991).

The contact with the overlying Ringerike Group is not exposed in the quarry. The underlying Braksøya Formation, consisting of patch reefs, crops out in its northwest corner at the foot of the quarry wall. Its contact with the Steinsfjorden Formation is conformable. The contact between the sedimentary rocks and the larvikite intrusion lies 3 km to the southeast.

At 40 m above the base of the Steinsfjorden Formation there is a 75 cm thick band of green-grey, silicate-rich rock. It is identifiable in the east- and west-facing walls of the quarry by its distinct colour contrast with the lighter coloured limestone (Fig. 2a). The band has a conformable relationship with the limestone and the upper and lower boundaries are clearly marked by 3-5 mm thick white calcite bands (Fig. 2a). The silicate-rich rock has three clearly identifiable sub-layers. These are each approximately 25 cm thick and their boundaries are also highlighted by colour changes and thinner bands of white calcite (Fig. 2a).

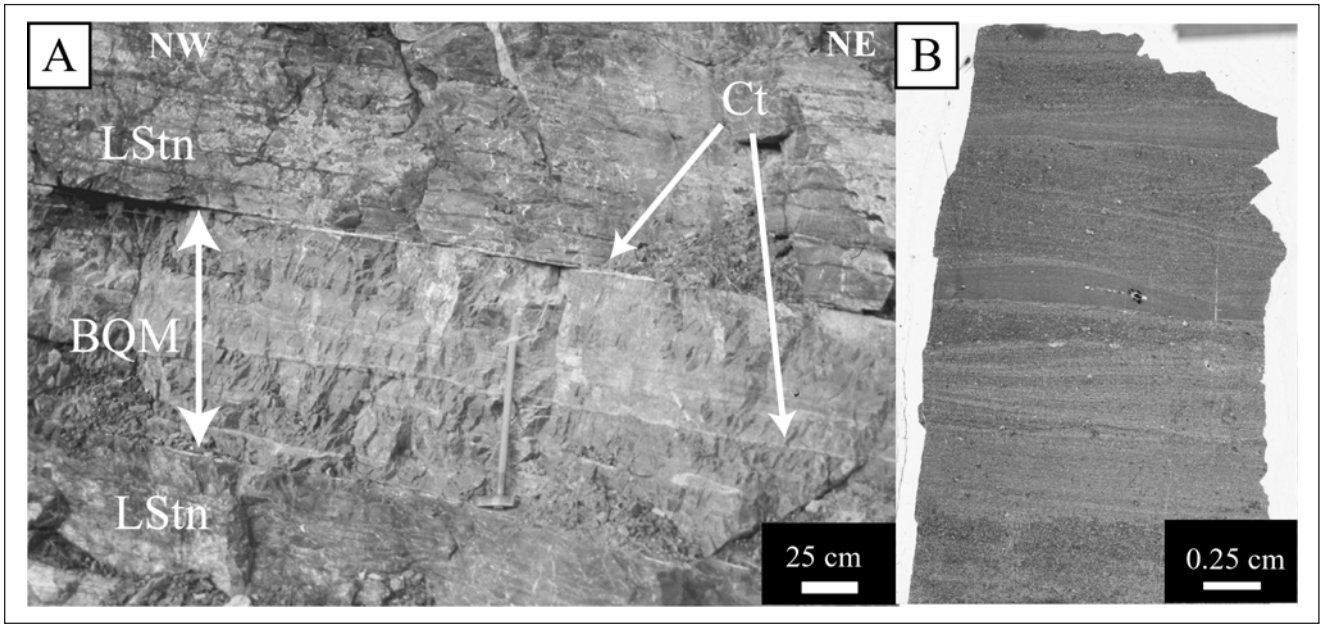

Fig. 2A: The Bjørntvet Quarry metabentonite (BQM) lies conformably in the limestone (LStn). The contacts are clearly depicted by recrystallised white calcite (Ct). Fig 2B: A thin section of the middle sub-layer displaying horizontal layering with cross-bedding structures (sample CJH BVB-M6; PMO 203.505).

The features of each sub-layer are broadly similar. Cross-bedding and distinct layering on a sub-centimetre scale are observed (Fig. 2b). The relative proportions of silicate minerals decrease from bottom to top, both in the layer as a whole, and within each individual sub-layer. Small curved fragments of microcrystalline calcite, identified as shelly fragments, are also seen in each layer. The concentration of these fragments increases from bottom to top in each sub-layer, and increases generally from bottom to top of the layer as a whole. No xenoliths of possible clastic origin are found.

Petrography, textures and microstructures

Mineralogically the three sub-layers are characterised by the mineral assemblage quartz + calcite + biotite + white-mica + epidote + orthoclase + plagioclase + pyrite + amphibole + pyroxene. Localised occurrences of prehnite and pumpellyite are also present.

The matrix is dominated by quartz and calcite. Calcite occurs as either fine-grained microcrystalline clusters attributed to shell material, which has been cemented during diagenesis or larger euhedral crystals with well-defined triple points indicating carbonate recrystallisation during metamorphism.

Large primary minerals, up to 0,6 mm in diameter, have been pseudomorphed by concentrically distributed calcite + quartz + epidote ± pumpellyite (Fig. 3A) (Table 1). These clusters are more common towards the bottom of each sub-layer.

Table 1. Representative chemical analyses of epidote and chlorite

	1	2	3	4	5	6	7	8
SiO_2	39.44	39.26	37.90	37.58	28.3	29.5	28.8	28.2
Al_2O_3	32.31	30.33	27.87	27.46	19.3	19.4	19.5	20.2
TiO_2	0.06	0.06	0.13	0.05	0.02	<0.03	<0.03	0.04
MnO	0.03	0.01	<0.06	0.01	0.15	0.10	0.15	0.15
Fe_2O_3	1.80	4.10	6.12	8.5	13.3	10.9	9.7	16.3
MgO	<0.18	0.02	0.131	0.08	24.8	26.6	27.0	21.4
Na_2O	0.02	0.01	0.004	<0.05	0.01	<0.05	<0.05	0.02
K_2O	<0.05	0.03	0.03	0.01	0.02	0.02	0.03	0.03
CaO	25.17	24.54	24.13	24.51	0.06	0.12	0.03	0.01
Total	98.84	98.37	96.32	96.815	85.87	86.57	85.16	86.46
Cations								
Ca	2.05	2.03	2.07	2.12	0.01	0.02	0.01	0.00
Na	0.00	0.00	0.00	0.00	0.00	0.00	0.00	0.01
K	0.00	0.00	0.00	0.00	0.01	0.01	0.01	0.01
Mg	0.00	0.00	0.02	0.01	7.44	7.81	8.02	6.47
Fe	0.11	0.26	0.1	0.57	2.24	1.80	1.61	2.76
Mn	0.00	0.00	0.00	0.00	0.03	0.02	0.03	0.03
Ti	0.00	0.00	0.01	0.00	0.00	0.00	0.00	0.01
$Al_{(oct)}$	2.89	2.76	2.62	2.48	2.28	2.30	2.31	2.56
$Al_{(tet)}$	-	-	-	-	2.30	2.20	2.26	2.27
Si	3.00	3.03	3.03	3.03	5.70	5.80	5.74	5.73
ΣCations	8.05	8.08	7.85	8.21	20.01	19.96	19.99	19.85

Notes: Analyses 1-4 – Epidote; and Analyses 5-8 – Chlorite. Idealised anion groups are assumed and stoichiometry calculated on the basis of 12.5 and 36 oxygen atoms respectively.

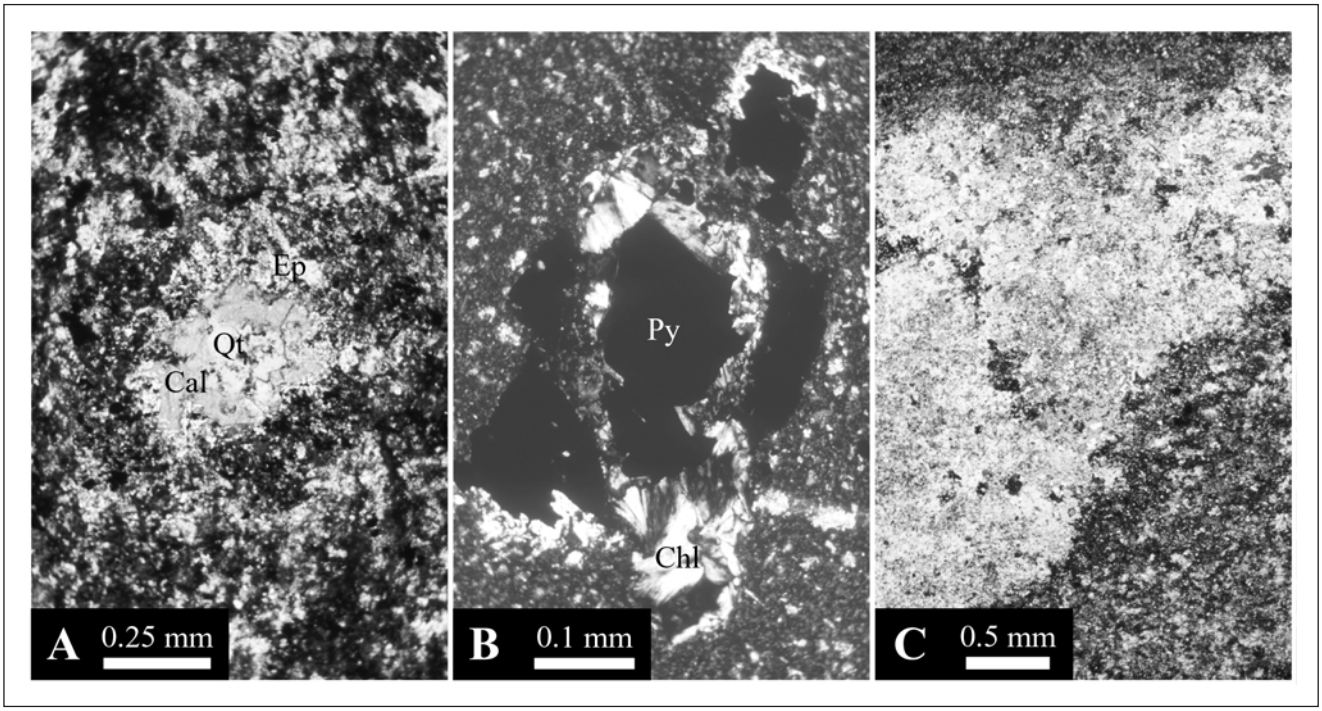

Fig. 3A: Photomicrograph of calcite + quartz + epidote pseudomorphing a primary igneous phenocryst (sample CJH BVB-B2; PMO 203.506). Fig. 3B: Photomicrograph of euhedral pyrite surrounded by chlorite (sample CJH BVB-M6; PMO 203.505). Fig. 3C: Horizontal bands of porphyroblastic diopside (sample CJH BVB-B; PMO 203.506)

Table 2. Representative chemical analyses of feldspars

	1	2	3	4	5	6	7	8	9	10	11	12	13
SiO_2	64.57	64.75	64.49	68.71	68.77	53.43	52.30	50.73	48.96	47.21	45.16	43.80	42.94
Al_2O_3	18.17	18.07	18.15	19.38	19.06	28.90	29.63	30.64	32.04	32.66	33.84	34.62	35.76
MnO	<0.06	<0.06	<0.06	0.03	0.05	<0.06	<0.06	0.08	0.02	0.02	<0.06	0.02	0.04
FeO	0.05	0.3	0.15	0.12	0.17	0.05	0.06	0.13	0.05	0.06	0.12	0.21	0.04
MgO	0.02	0.02	0.01	<0.18	<0.18	0.05	<0.18	0.29	0.02	<0.18	0.02	<0.18	<0.18
Na_2O	0.40	0.29	0.35	11.78	11.96	4.73	4.24	3.33	2.42	1.80	0.98	0.66	0.37
K_2O	16.11	16.22	16.1	0.18	0.41	0.47	0.62	0.80	0.85	0.28	0.33	<0.05	0.07
CaO	0.09	0.02	0.19	0.16	0.23	11.50	12.62	13.82	15.41	16.31	17.25	18.91	19.45
Total	99.45	99.68	99.46	100.36	100.67	99.13	99.46	99.81	99.76	98.34	97.71	98.23	98.67
Cations													
Ca	0.00	0.00	0.01	0.01	0.01	0.56	0.62	0.68	0.76	0.81	0.87	0.95	0.98
Na	0.04	0.03	0.03	1.00	1.01	0.42	0.38	0.30	0.22	0.16	0.09	0.06	0.03
K	0.95	0.96	0.96	0.01	0.02	0.03	0.04	0.05	0.05	0.02	0.02	0.00	0.00
Mg	0.00	0.00	0.00	0.00	0.00	0.00	0.00	0.02	0.00	0.00	0.00	0.00	0.00
Fe	0.00	0.01	0.01	0.00	0.01	0.00	0.00	0.00	0.00	0.00	0.00	0.01	0.00
Mn	0.00	0.00	0.00	0.00	0.00	0.00	0.00	0.00	0.00	0.00	0.00	0.00	0.00
Al	1.00	0.99	0.99	1.00	0.98	1.55	1.60	1.65	1.74	1.79	1.88	1.92	1.98
Si	3.00	3.00	3.00	3.00	3.00	2.44	2.39	2.32	2.25	2.20	2.13	2.06	2.02
ΣCations	4.99	4.99	5.00	5.02	5.03	5.00	5.03	5.02	5.02	4.98	4.99	5.00	5.01

Notes: Analyses 1-3 – Orthoclase; and Analyses 4-13 – Plagioclase. Stoichiometry calculated on the basis of 8 oxygen atoms.

Crystals of pyrite (>0.4 mm) (Figure 3B) are found at the centre of corona structures rimmed by chlorite (Table 1). There is no structure associated with pyrite to indicate whether its origin is biogenic or lithogenic.

Orthoclase (Or_{91-98}) is found as a rock-forming mineral (Table 2; analyses 1-2), or occasionally as inclusions in epidote around pyrite blasts (Table 2; analysis 3). Plagioclase occurs either as a reaction product

Table 3. Representative chemical analyses of tremolite and diopside

	1	2	3	4	5	6	7	8
SiO_2	51.55	53.42	56.12	55.49	52.61	53.79	53.42	52.34
Al_2O_3	3.77	2.98	1.15	1.01	1.09	0.26	0.26	0.02
TiO_2	0.19	0.11	<0.03	0.03	<0.03	<0.03	0.02	<0.03
MnO	0.12	0.10	0.12	0.15	0.36	0.13	0.10	0.29
Fe_2O_3	8.36	7.39	5.45	7.71	7.91	5.68	6.14	10.82
MgO	18.19	19.10	21.24	19.41	13.03	14.75	14.40	11.36
Na_2O	0.43	0.33	0.09	0.11	0.04	0.07	0.03	0.02
K_2O	0.38	0.24	0.03	0.04	0.02	0.01	<0.05	<0.05
CaO	13.03	13.50	13.43	13.40	24.23	24.89	25.08	24.43
Cr_2O_3	n.a.	n.a.	n.a.	n.a.	0.03	0.11	0.14	<0.06
Total	96.01	97.18	97.64	97.34	99.35	99.68	99.59	99.28
Cations								
Ca	2.02	2.05	2.00	2.03	0.98	0.99	1.00	1.00
Na	0.12	0.09	0.03	0.03	0.00	0.00	0.00	0.00
K	0.07	0.04	0.01	0.01	0.00	0.00	0.00	0.00
Mg	3.93	4.04	4.41	4.09	0.73	0.82	0.80	0.65
Fe	1.01	0.88	0.64	0.91	0.25	0.18	0.19	0.35
Mn	0.01	0.01	0.01	0.02	0.01	0.00	0.00	0.01
Cr	n.a.	n.a.	n.a.	n.a.	0.00	0.00	0.00	0.00
Ti	0.02	0.01	0.00	0.00	0.00	0.00	0.00	0.00
$Al_{(oct)}$	0.11	0.08	0.01	0.01	0.03	0.01	0.00	0.00
$Al_{(tet)}$	0.54	0.41	0.18	0.16	0.02	0.00	0.01	0.00
Si	7.46	7.59	7.82	7.84	1.98	2.00	1.99	2.00
ΣCations	15.29	15.20	15.11	15.10	4.00	4.00	3.99	4.01

Notes: Analyses 1-4 – Tremolite; and Analyses 5-8 – Diopside. Idealised anion group assumed for tremolite. Stoichiometry calculated on the basis of 23 and 8 oxygen atoms respectively. n.a. – Not Analysed.

Table 4. Representative chemical analyses of biotite and muscovite

	1	2	3	4	5
SiO_2	41.46	40.12	42.01	49.21	49.39
Al_2O_3	15.14	15.59	14.53	30.58	30.61
TiO_2	0.55	0.50	0.46	0.08	0.09
Cr_2O_3	<0.06	<0.06	0.08	<0.06	<0.06
MnO	0.04	<0.06	0.08	0.03	<0.06
FeO	8.03	7.96	7.12	2.09	2.19
MgO	19.89	19.67	20.37	3.95	3.94
Na_2O	0.06	0.07	0.10	0.21	0.17
K_2O	9.31	9.48	9.41	10.00	9.80
CaO	0.23	0.07	0.14	0.01	0.02
Total	94.71	93.48	94.29	96.17	96.21
Cations					
Ca	0.04	0.01	0.02	0.00	0.00
Na	0.02	0.02	0.03	0.05	0.04
K	1.71	1.77	1.72	1.68	1.65
Mg	4.26	4.28	4.36	0.78	0.77
Fe	0.96	0.97	0.86	0.23	0.24
Mn	0.00	0.00	0.01	0.00	0.00
Cr	0.00	0.00	0.01	0.00	0.00
Ti	0.06	0.05	0.05	0.01	0.01
$Al_{(oct)}$	0.52	0.54	0.50	3.24	3.25
$Al_{(tet)}$	2.04	2.14	1.96	1.51	1.50
Si	5.96	5.86	6.04	6.49	6.50
Σ Cations	15.57	15.64	15.56	13.99	13.96

Notes: Analyses 1-3 – Biotite; and Analyses 4-5 – Muscovite. Idealised anion groups are assumed and stoichiometry calculated on the basis of 22 oxygen atoms.

around tremolite (Table 3; analyses 1-4) where it has an Ab_{100} composition (Table 2; analyses 4-5), or as a rock-forming mineral in the matrix where it has a range of compositions (An_{56-98}; Table 2; analyses 6-13).

Diopside (Di_{65-85}; Table 3; analyses 5-8) occurs as 5 mm thick horizontal bands of poikiloblasts. The bands have a near-continuous presence across thin sections. The blasts contain inclusions that characterise the fine-grained rock-forming sedimentary matrix, indicating that the diopside grew after deposition and is metamorphic.

Biotite and muscovite (Table 4) are found as minor phases in the rock-forming matrix. They are chemically homogeneous and very fine-grained. The biotite is enriched in Mg relative to Fe, has a low $Al_{(tet)}$ content and a $Si:Al_{(tot)}$ ratio approaching 3:1. Its size and composition suggests that it is metamorphic (Guidotti 1984). This observation is supported by the difference in its composition compared to biotite phenocrysts in north European and Scandinavian bentonites (Batchelor 2003) and to magmatic biotites (Abdel-Rahman 1994).

Small veinlets (1-2 cm) cut the sedimentary structures perpendicular to the bedding surfaces. The veinlets are filled with calcite and prehnite. Larger, vertically orientated cracks and fractures are found in the limestone directly above and below the silicate layer. These fractures contain calcite, analcite and chabazite.

This silicate layer is believed to represent an altered volcanic ash or metabentonite. It is argued that the original sediments were clay minerals derived from volcanic ash and glass, and sedimentary calcite, which were deposited together during a volcanic eruption in the Late Wenlock/Early Ludlow. The rock was later metamorphosed during emplacement of the Permian larvikite complex.

Table 5. Major oxide and trace element concentrations

	BOTTOM	MIDDLE	TOP
Na_2O	0.87	1.29	0.39
MgO	4.05	3.21	1.61
Al_2O_3	19.67	19.06	9.52
SiO_2	48.44	52.44	31.48
P_2O_5	0.32	0.16	0.09
SO_3	0.49	0.55	0.85
K_2O	4.71	6.51	3.27
CaO	12.53	10.24	29.20
TiO_2	0.60	0.62	0.28
MnO	0.04	0.03	0.08
Fe_2O_3	3.04	2.24	1.65
LOI	5.3	3.7	21.7
Total	100.06	100.05	100.12
V	130	120	108
Cr	59	46	41
Co*	6	5	5
Ni	6	5	6
Cu	10	8	9
Zn	460	93	60
Ga	20	18	11
As*	7	4	3
Br	1	2	1
Rb	119	169	109
Sr	388	476	578
Y	36	30	26
Zr	349	396	200
Nb	18	18	11
Mo	2	1	< 0.5
Sn	3	1	1
Sb*	0.2	0.14	0.1
Ba	224	301	132
La*	27.8	26.8	18.8
Ce*	55.8	52.2	37.4
Pr	10	16	< 1.8
Nd*	27.4	24	18.7
Sm*	5	4	4
Eu*	0.9	0.7	0.9
Tb*	0.4	0.4	0.4
Yb*	0.6	0.5	0.8
Lu*	0.13	<0.1	<0.1
Hf	7	8	4
Pb	26	38	23
Th	19	19	13
U	6	5	4

*Major oxide concentrations in wt.% and trace element concentrations in ppm.*Denotes element analysed by ICP-MS. LOI = Loss on Ignition. (BOTTOM – sample CJH-BVB-B; PMO 203.508. MIDDLE – sample CJH-BVB-M; PMO 203.509. TOP – sample CJH-BVB-T; PMO 203.510)*

Biostratigraphy

The growth of metamorphic diopside suggests temperatures of at least 300°C were reached during metamorphism (Bucher & Frey 1994). As a result most fossil elements that may have existed have been altered or destroyed making the application of biostratigraphy difficult.

A reef-like structure has been identified 250 m to the east of the quarry. Its stratigraphical position is close to the top of the Steinsfjorden Formation. The reef contains many examples of macrofossils, including sponges, brachiopods, corals, crinoids and bryozoans, but no microfossil elements were found to provide a conclusive age (sample CJH-PG0206; PMO 203.511). At present the upper boundary of the Steinsfjorden Formation in this area is poorly constrained (Davies 2003).

Two samples of limestone from above (20 cm and 65 cm) and two from below (20 cm and 65 cm) the metabentonite were crushed to fragments of <3 cm and dissolved in weak (8-10 %) formic acid. Formic acid was preferred to acetic acid to ensure more complete dissolution of the metamorphosed carbonate rock. The residues were sieved and the 63-500 μm fractions placed in bromoform heavy liquid. Both the heavy and the light fractions were hand-picked for phosphatic and other microfossil components.

The two samples from above the metabentonite bed were barren and no microfossil elements were found. The sample 65 cm below the metabentonite yielded a Pa element of *Ozarkodina* cf. *excavata* (Fig. 4A), and an *Oulodus* sp. element (Fig. 4B). From the sample 20 cm below the metabentonite a simple cone conodont *Panderodus* sp., a Pb element of *Ozarkodina* cf. *confluens* (Fig. 4C), and an *Ozarkodina* sp. fragment were identified. The conodonts are dark brown in colour indicating that they were heated to more than 300°C (Epstein et al. 1977), confirming the temperatures predicted from the metamorphic mineral assemblage.

Colour alteration of conodonts due to intrusions in the Oslo region is well-documented (Aldridge 1984). The highest conodont alteration index values are generally from localities adjacent to the Permian intrusions, and the lowest values are from areas further away from these intrusions. Proximity to Permian intrusions better explains the observed thermal effects on our conodont elements. Burial has played a less pronounced role.

In addition to conodonts, elements of scolecondonts (polychaete worm jaws) were also found (Fig. 4D-G). The investigated MI elements may belong to a single species of the family Paulinitidae. Their precise taxonomic placement is uncertain, but they may belong

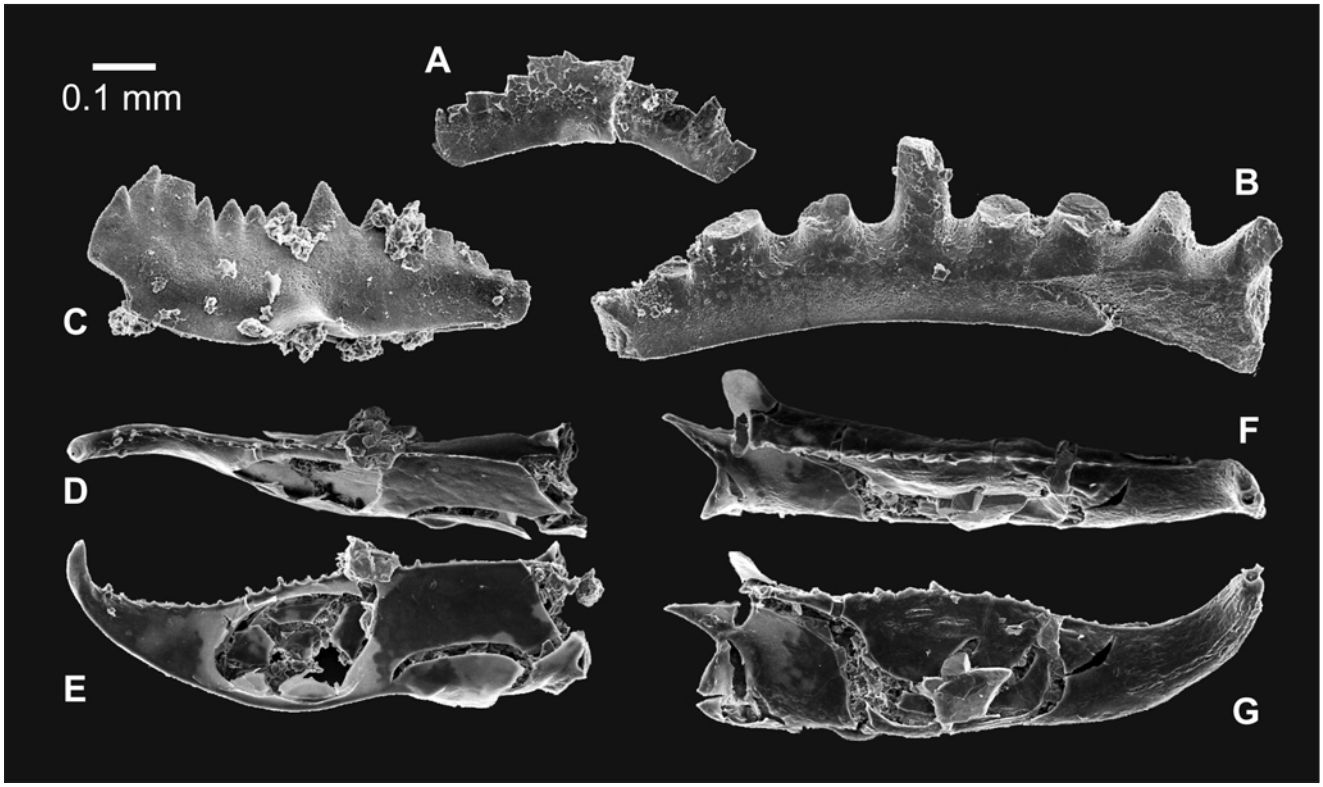

Fig. 4: Microfossil elements from 20 and 65 cm below the metabentonite. A - Ozarkodina cf. *excavata (Branson & Mehl 1933), Pb element (PMO 203.500); B - Conodont Oulodus* sp. *(PMO 203.501); C – Ozarkodina* cf. *Confluens (Branson & Mehl 1933), Pa element (PMO 203.502); D & E – Scolecondont indet. specimen A, MI element (PMO 203.503); F & G – Scolecondont indet. specimen B, MI element (PMO 203.504). All illustrated specimens are housed in the collections of the Geological Museum, University of Oslo.*

to *Hindenites*, *Kettnerites* or a new genus (Bergman, Eriksson, pers. comm. 2003). The two genera are well known from Wenlock and Ludlow strata of Gotland (Sweden) (Bergman 1989), but cannot be used to refine the biostratigraphy of the investigated samples. This is the first reported occurrence of scolecondonts from the Cambro-Silurian of the Oslo Region.

Geochemistry

In contrast to the under- and overlying limestone, which has a bulk-average ignited CaO content of >60 wt.%, the metabentonite layer contains significant quantities of SiO_2, Al_2O_3, MgO, K_2O and Fe_2O_3 (Table 5). Considerable variations between each of the three sub-layers are also recorded. Generally, the CaO content increases from bottom to top. A smaller increase is also recorded in the SO_3 content. This may reflect an increasing biogenic component being deposited along with the silicate material, or post-depositional bioturbation.

It must be assumed that the original mineralogy of the rock has been considerably altered since deposition. The original ashes and volcanic glass were altered to clay, with unquantifiable interaction between the material and seawater during deposition and later thermal metamorphism. Therefore, any meaningful investigation of the chemistry of the rocks may only be approached through the use of selected element ratios.

Bentonite clays form through the alteration of silicic ash by prolonged contact with seawater in conditions of low SiO_2 activity. Predominant clay-forming elements, such as Si and Al, may be used in conjunction with Ti to test the precursor material of the clays. It has been shown that clays with a volcanic origin have lower SiO_2/Al_2O_3 concentrations than clays with a detrital origin (Teale & Spears 1986). Using data presented by Batchelor et al. (1995) the Bjørntvet Quarry samples have low TiO_2/Al_2O_3 ratios, and relatively low SiO_2/Al_2O_3 ratios. These ratios are characteristic of other Scandinavian bentonite clays (Fig 5).

Trace element ratios may be used to discriminate between different volcanic rock types. Amongst those most commonly applied are Nb/Y (an index of alkalinity) and Zr/TiO_2 (an index of differentiation) (Winchester & Floyd 1977). The trace element chemistry of our samples shows them to have a sub-alkaline/calc-alkaline affinity and a differentiation index common to dacites (Fig. 6).

Trace element ratios are also used as discrimination factors for the tectonic interpretation of subvolcanic

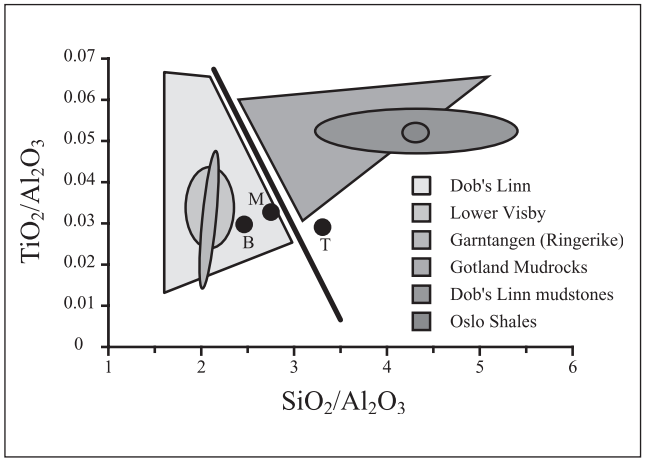

Fig. 5: Discrimination diagram for detrital and volcanogenic clay rocks based on SiO_2/Al_2O_3 and TiO_2/Al_2O_3 ratios.

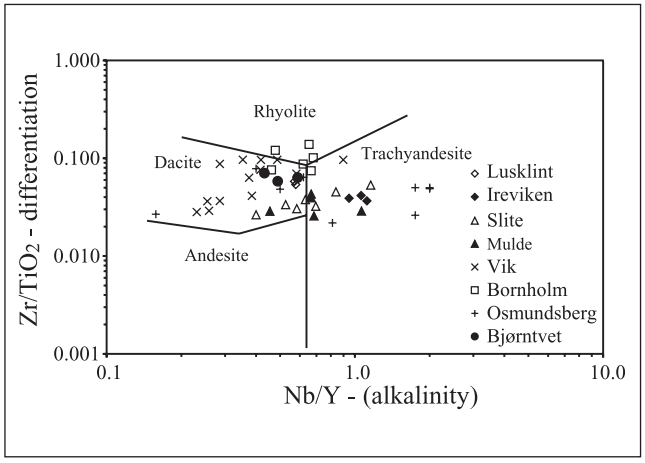

Fig. 6: Metabentonite data plotted on the Nb/Y vs. Zr/TiO_2 geochemical grid of Winchester & Floyd (1977). Data from Batchelor & Jeppsson (1994); Batchelor & Jeppsson (1999); Batchelor et al. (1995); Huff et al. (1997); Obst et al. (2002).

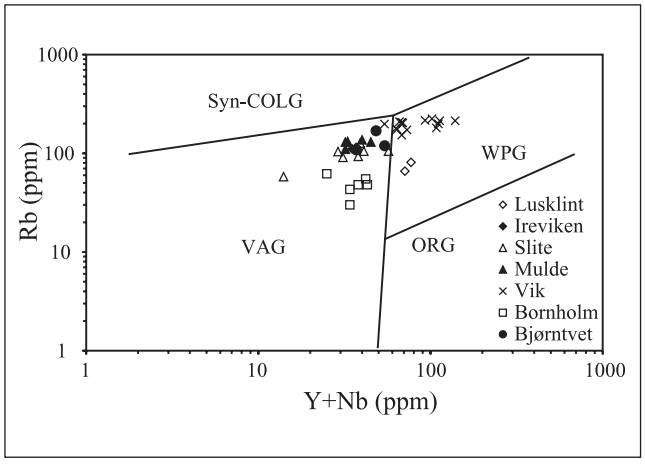

Fig. 7: Metabentonite data plotted on the tectonic discrimination diagrams for granites and alkali granites (Pearce et al., 1984). WPG = within-plate granite; ORG = ocean ridge granite; VAG = volcanic arc granite; Syn-COLG = syn-collision granite. Data from Batchelor & Jeppsson (1994); Batchelor & Jeppsson (1999); Batchelor et al. (1995); Huff et al. (1997); Obst et al. (2002).

granites and alkali granites (Pearce et al. 1984). The eruptive equivalents of these granites are alkaline and peralkaline volcanics, and while the discrimination diagrams were not designed for such rocks senso stricto, they have been widely applied (e.g. Merriman & Roberts 1990; Pearce 1995) and provide a useful technique for indicating tectonic settings and comparing and contrasting different bentonite chemistries (Fig 7). The Bjørntvet Quarry samples have a chemistry similar to rocks associated with a volcanic arc type setting.

The chondrite-normalised rare earth element (REE) patterns for the three samples are quite similar and display light REE-enriched profiles with very weak, negative Eu anomalies (Fig. 8a). A MORB-normalised pattern for selected trace elements shows strong positive anomalies for Rb, K, Th and Zr and negative anomalies for Ti, Ni and Cr (Fig 8b).

Discussion

The 75 cm thick green-grey silicate-rich horizon at the Bjørntvet Quarry is continuously exposed across a 1.5 km face of limestone. The lighter-coloured, 115 m thick limestone contains significantly less silicate material than the green-coloured horizon of interest. There is no evidence of any clastic sedimentation in the limestone or in the silicate-rich horizon.

The fine-grained metamorphic mineral assemblage contains appreciable quantities of potassic minerals, pseudomorphed blasts and poikiloblasts. Despite recrystallisation, there is clear evidence that the unit was deposited in a sedimentary environment, and not intruded (Fig 3B). The dark brown colour of the conodonts supports this; when found directly adjacent to an intrusion a conodont's colour is altered from dark brown to grey or white (Epstein et al. 1977). The transition between the limestone and the silicate-rich horizon is conformable and sharp (Fig 3A). There is no evidence of a transition between the shallow waters associated with limestone deposition and the deeper benthic environments associated with clays and shales that would indicate a temporary change in the sedimentary environment.

Conodonts have not previously been reported from the Upper Wenlock rocks of the Oslo Region, but a well established conodont biostratigraphy exists for the underlying Llandovery series (Aldridge & Mohamed 1982). The conodonts *Ozarkodina confluens* and *Ozarkodina excavate* are common species in the Silurian (Wenlock – Lower Ludlow) of Sweden (Gotland), Estonia and elsewhere. *Ozarkodina confluens* has a slightly wider stratigraphic range, and may reach to the

top of the Ludlow (Jeppsson et al. 1994). On the basis of these two conodonts, the age of the limestone immediately below the metabentonite cannot be more precisely dated than Late Wenlock to Early Ludlow.

Sanidine phenocrysts are common in volcanic calc-alkaline rocks, and have been reported in several Palaeozoic bentonites in Scandinavia (Kiipli & Kallaste 2002) and are often of value in characterising volcanic rocks (Weaver 1963). The large pseudomorphs containing quartz + calcite + epidote ± pumpellyite (Fig. 3A) are interpreted to be sanidine phenocrysts that were replaced by the observed assemblage during burial and thermal metamorphism.

Geochemically the silicate-rich rocks have a calc-alkaline signature (Fig. 6) and can be discriminated on the basis of their trace element ratios as being similar to volcanic arc granites (Fig. 7). Trace element and rare earth element normalisation plots show that they are similar to many examples of evolved igneous rocks. Specifically, the enrichment of incompatible elements (Rb, K, Th and Zr) and depletion of elements typically enriched in basalts (Ti, Ni and Cr) is further evidence for derivation from an evolved magma source (Fig. 8).

The lack of tightly constrained fossil assemblages in rocks from the southern Oslo Region is responsible for great uncertainty as to the stratigraphic position of the Bjørntvet metabentonite. The lower sections of the Steinsfjorden Formation at Holmestrand have a Sheinwoodian appearance (Worsley et al. 1983), while the top of the Formation marks the Wenlock/Ludlow boundary. Several bentonites, from both the Oslo Region and further afield in Scandinavia, have been reported from rocks falling within these age limits (Table 6). In the Oslo Region, two bentonites are reported in the Steinsfjorden Formation near Ødegårdsviken (Jørgensen 1964), the younger of which may be correlated with a single bentonite at Åsa in the Brattstad Member of the formation (Whitaker 1977; Worsley et al. 1983). Elsewhere, Upper Wenlock metabentonites have been identified in the Slite and Mulde formations on Gotland (Batchelor & Jeppsson 1999) and the Cyrtograptus Shale on Bornholm, Denmark (Obst et al. 2002).

Chemical data for the Åsa or Ødegårdsviken bentonites are not available; hence geochemical correlation between them and the rocks from the Bjørntvet Quarry can not be made. The bentonites from the Mulde and Slite formations on Bornholm and in the Bjørntvet Quarry plot in the same compositional field (Fig. 6), and they may all have evolved in a volcanic arc type tectonic setting (Fig. 7). However, a log-log plot of several trace element ratios (Fig. 9) shows that correlation between the rocks is poor.

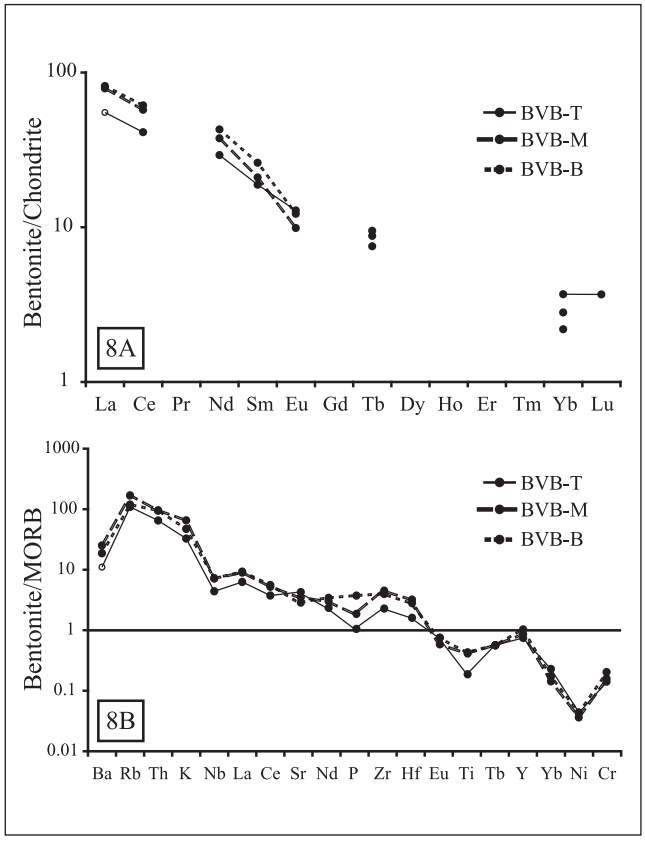

Fig. 8A: Chondrite-normalised rare earth element (REE) data for the Bjørntvet Quarry metabentonites. Normalising values from Wakita et al. (1971).
Fig. 8B: MORB-normalised trace and rare earth element data for the Bjørntvet Quarry metabentonites. Normlising values from Saunders & Tarney (1984).

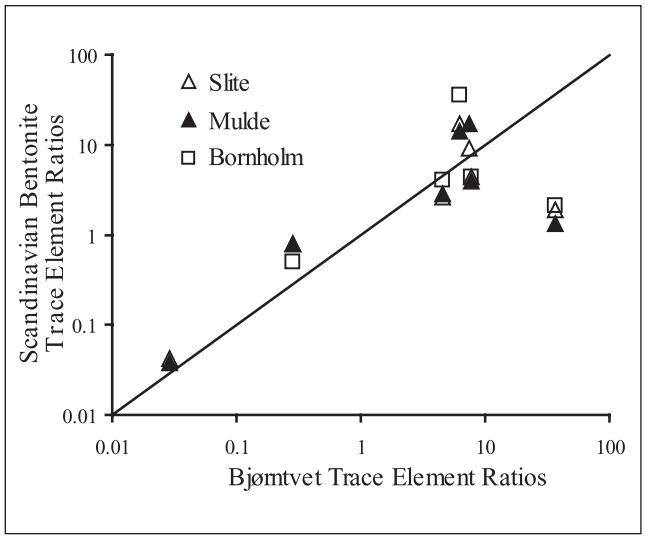

Fig. 9: Log-log plot of some trace element ratios for the bentonites of Bjørntvet (this study), Bornholm (Obst et al. 2002) and the Mulde and Slite Formations of Gotland (Batchelor & Jeppsson 1999). Ratios plotted: Rb/Sr, TiO_2/Th, Zr/Nb, Ce/Y, Zn/Ni, V/Ga and Ba/Pb.

Table 6. Stratigraphic distribution of bentonites in Scandinavia

Age	Unit	Equivalent Graptolite Zone	Locality	
Wenlock	*Homerian*	*ludensis*	*Mulde Formation (Batchelor & Jeppsson 1999)*	?
		lundgreni	*Åsa (Worsley et al., 1983)* *Ødegårdsviken – 9f/g (Jørgensen 1964)* *Bornholm (Obst et al. 2002)*	***Bjørntvet metabentonite***
	Sheinwoodian	*ellesae*	*Slite Formation (Batchelor & Jeppsson 1999)*	
		linnarssoni	*Ødegårdsviken – 9c (Jørgensen 1964)*	?
Llandovery	*Telychian*	*crenulata*	*Visby Formation (Batchelor & Evans 2000)*	
		crispus	*Vik, Ringerike (Batchelor et al. 1995)*	
	Fronian	*sedgwickii*	*Osmundsberg (Huff et al. 1997)*	

Conclusions

The sedimentological, petrographical and geochemical characteristics of the silicate-rich horizon in the Bjørntvet Quarry suggest that it is a metamorphosed bentonite. There is evidence that the silicates were deposited in a marine sedimentary environment. There is no evidence that they were intruded, or that they are related to any intrusive rock of the larvikite complex.

The chemical signatures of the rocks indicate that the volcanics were erupted from a volcanic arc related tectonic environment. The source of the volcanics was from evolved and calc-alkaline magma with a dacitic composition. This, in turn could have been related to closure along the Tornquist line in the latter half of the Silurian (Cocks & Torsvik 2002).

The rocks immediately overlying the Steinsfjorden Formation at Bjørntvet belong to the Holmestrand Formation of the Ringerike Group and are generally considered to mark the beginning of the Ludlow. This observation and the limited micropalaeontological evidence collected from the limestone dates the rock to being no older than Late Wenlock.

The uncertainty regarding the Bjørntvet metabentonite's biostratigraphic position does not allow direct correlation between it and two previously reported Upper Wenlock bentonites from Åsa and Ødegårdsviken in the Oslo Region. Nor are there any distinctive geochemical discrimination functions that allow correlation with stratigraphically similar bentonites from across Scandinavia. More detailed geochemical and mineralogical characterisation of bentonites in rocks from stratigraphically similar localities should be pursued and the application of more powerful geochemical techniques (e.g. REE analysis in apatite crystals) may also be beneficial for improving correlation between these rocks and other metabentonitic horizons in northern Europe.

Acknowledgements: We thank Norcem AS Brevik for providing access to the Bjørntvet Quarry during fieldwork and Andreas Harstad for field assistance and comments on an earlier version of this manuscript. David Worsley and Nils Spjeldnas are thanked for their helpful reviews.

References

Abdel-Rahman, A.-F. M. 1994: Nature of biotites from alkaline, calc-alkaline and peraluminous magmas. *Journal of Petrology 35*, 525-541.

Aldridge, R. J. 1984: Thermal metamorphism of the Silurian strata of the Oslo Region, assessed by conodont colour. *Geological Magazine 121*, 347-349.

Aldridge, R. J. & Mohamed, I. 1982: Conodont biostratigraphy of the Early Silurian of the Oslo Region. In Worsley, D. (ed): *IUGS Subcommission on Silurian Stratigraphy, Field Meeting, Oslo Region. Paleontological contributions from the University of Oslo*, 109-120, University of Oslo.

Batchelor, R. A. 1999: Metabentonites from the Silurian inliers of the southern Midland Valley of Scotland: distribution and geochemistry. *Scottish Journal of Geology 35*, 71-77.

Batchelor, R. A. 2003: Geochemistry of biotite in metabentonites as an age discriminant, indicator of regional magma sources and potential correlating tool. *Mineralogical Magazine 67*, 807-817.

Batchelor, R. A. & Evans, J. 2000: Use of strontium isotope ratios and rare earth elements in apatite microphenocrysts for characterization and correlation of Silurian metabentonites: a Scandinavian case study. *Norsk Geologisk Tidsskrift 80*, 3-8.

Batchelor, R. A. & Jeppsson, L. 1994: Late Llandovery bentonites from Gotland, Sweden, as chemostratigraphic markers. *Journal of the Geological Society, London 151*, 741-746.

Batchelor, R. A. & Jeppsson, L. 1999: Wenlock metabentonites from Gotland, Sweden: geochemistry, sources and potential as chemostratigraphic markers. *Geological Magazine 136*, 661-669.

Batchelor, R. A., Weir, J. A. & Spjeldnæs, N. 1995: Geochemistry of Telychian metabentonites from Vik, Ringerike District, Oslo Region. *Norsk Geologisk Tidsskrift 75*, 219-228.

Bergman, C. F. 1989: Silurian paulinitid polychaetes from Gotland. *Fossils and Strata 25*, 128.

Branson, E. B. & Mehl, C. C. 1933: Conodont studies no. 1: Conodonts from the Harding sandstone of Colorado; Bainbridge(Silurian) of Missouri; Jefferson City (Lower Ordovician) of Missouri. *University of Missouri Studies 8*, 5-72.

Bucher, K. & Frey, M. 1994: *Petrogenesis of metamorphic rocks.* Springer-Verlag Berlin.

Cocks, L. R. M. & Torsvik, T. H. 2002: Earth geography from 500 to 400 milliion years ago: a faunal and palaeomagnetic review. *Journal of the Geological Society, London 159*, 631-644.

Davies, N. S. 2003: The Ringerike Group (Late Silurian, Oslo Region): Palaeoenvironmental analysis of an Old Red Sandstone sequence in the foreland basin of the Norwegian Caledonides. *Unpub. Ph.D. Thesis, University of Birmingham, Birmingham.*

Epstein, A. G., Epstein, J. B. & Harris, L. D. 1977: Conodont color alteration - An index to organic metamorphism. *U.S. Geological Survey Professional Paper 995*, 27 p.

Fortey, N. J., Merriman, R. K. & Huff, W. D. 1996: Silurian and late Ordovician K-bentonites as a record of late Caledonian volcanism in the British Isles. *Transactions of the Royal Society Edinburgh Earth Sciences 86*, 167-180.

Guidotti, C. V., 1984: Micas in metamorphic rocks. In Bailey, S. (ed): *Reviews in Mineralogy*. Mineralogical Society of America, Washington, 584 pp.

Huff, W. D., Bergström, S. M., Kolata, D. R. & Sun, H. 1997: The Lower Silurian Osmundsberg K-bentonite. Part II: Mineralogy, geochemistry, chemostratigraphy and tectonomagmatic significance. *Geological Magazine 135*, 15-26.

Jeppsson, L., Viira, V. & Männik, P. 1994: Silurian conodont-based correlations between Gotland (Sweden) and Saaremaa (Estonia). *Geological Magazine 131*, 201-218.

Jørgensen, P. 1964: Mineralogical composition of two Silurian bentonite beds from Sundvollen, Southern Norway. *Norsk Geologisk Tidsskrift 44*, 227-234.

Kiipli, T. & Kallaste, T. 2002: Correlation of Telychian sections from shallow to deep sea facies in Estonia and Latvia based on the sanidine composition of bentonites. *Proceedings of the Estonian Academy of Sciences – Geology 51*, 143-156.

Kiipli, T., Männik, P., Batchelor, R. A., Kiipli, E., Kallaste, T. & Perens, H., 2001: Correlation of Telychian (Silurian) altered volcanic ash beds in Estonia, Sweden and Norway. *Norsk Geologisk Tidsskrift 81*, 179-194.

Kretz, R 1983: Symbols for rock-forming minerals. *American Mineralogist 68*, 277-279

Merriman, R. K. & Roberts, B. 1990: Metabentonites in the Moffat Shale Group, Southern Uplands of Scotland: Geochemical evidence of ensialic marginal basin volcanism. *Geological Magazine 127*, 259-271.

Obst, K., Böhnke, A., Katzung, G. & Maletz, J. 2002: Pb-Pb zircon dating of tuff horizons in the Cyrtograptus Shale (Wenlock, Silurian) of Bornholm, Denmark. *Bulletin of the Geological Society of Denmark 48*, 1-8.

Pearce, J. A., Harris, N. B. W. & Tindle, A. G. 1984: Trace element discrimination diagrams for the Tectonic Interpretation of Granitic Rocks. *Journal of Petrology 25*, 956-983.

Pearce, R. B. 1995: The geochemistry of Llandovery and Wenlock age K-bentonites in the Southern Uplands. *Scottish Journal of Geology 31*, 23-28.

Pouchou, J. L. & Pichoir, F. 1984: A new model for quantitative X-ray microanalysis. Part I: application to the analysis of homogeneous samples. *La Recherche Aerospatiale*, 13-38.

Saunders, A. D. & Tarney, J. 1984: Geochemical characteristics of basaltic volcanism within back-arc basins. *In* Kokelaar, B. P. & Howells, M. F. (eds): *Marginal Basin Geology. Geological Society Special Publication.* Blackwell Scientific Publications, 322 pp.

Teale, C. T. & Spears, D. A. 1986: The mineralogy and origin of some Silurian bentonites, Welsh Borderland, U.K. *Sedimentology 33*, 757-765.

Wakita, H., Rey, P. & Schmitt, R. A. 1971: Abundances of the 14 rare-earth elements and 12 other trace elements in Apollo 12 samples: Five igneous and one breccia rocks and four soils. *Proceedings of the Second Lunar Science Conference 2*, 1319-1329.

Weaver, C. E., 1963: Interpretive value of heavy minerals from bentonites. *Journal of Sedimentary Petrology 33*, 342-349.

Whitaker, J.H. McD. 1977: *A guide to the Geology around Steinsfjorden, Ringerike.* Universitetsforlaget, Oslo, 56 pp.

Wilkinson, J. B. 1991: A facies analysis of the Steinsfjorden Formation (Wenlock Series) within two areas of southeast Norway. *Unpublished Ph.D. Thesis, Portsmouth Polytechnic, Portsmouth.*

Winchester, J. A. & Floyd, P. A. 1977: Geochemical discrimination of different magma series and their differentiation products using immobile elements. *Chemical Geology 20*, 325-343.

Worsley, D., Aarhus, N., Bassett, M. G., Howe, M. P. A., Mørk, A. & Olaussen, S. 1983: The Silurian succession of the Oslo Region. *Norges Geologiske Undersøkelse Bulletin 384*, 57 pp.